eye disc (5) may thus be visualized as expanding concentric rings of dp-ERK.

In accordance with the multiple functions of DER during development, many of the dp-ERK patterns are attributed to DER activation. The temporal and spatial correlation of DER-induced dp-ERK to Rho expression stands out. The only exception is the activation of DER in the ventral ectoderm at stage 10 that is induced by Spitz-processing machinery restricted to the midline. These findings point to Rho as the limiting element in activation of the DER pathway. Different ranges of diffusion were observed for Spitz in different biological contexts, highlighting the importance of molecules that may restrict or facilitate ligand diffusion in regulating the spatial pattern of receptor activation.

REFERENCES AND NOTES

1. R. Seger and E. G. Krebs, *FASEB J.* **9**, 726 (1995).
2. R. Schweitzer and B.-Z. Shilo, *Trends Genet.* **13**, 191 (1997).
3. E. Raz and B. Z. Shilo, *Genes Dev.* **7**, 1937 (1993).
4. F. J. Diaz-Benjumea and A. Garcia-Bellido, *Proc. R. Soc. London Ser. B* **242**, 36 (1990).
5. M. Freeman, *Cell* **87**, 651 (1996).
6. M. Tio and K. Moses, *Development* **124**, 343 (1997).
7. T. Schüpbach, *Cell* **49**, 699 (1987); A. González-Reyes, H. Elliot, D. St. Johnston, *Nature* **375**, 654 (1995); S. Roth, F. S. Neuman-Silberberg, G. Barcelo, T. Schüpbach, *Cell* **81**, 967 (1995).
8. R. Schweitzer, M. Shaharabany, R. Seger, B.-Z. Shilo, *Genes Dev.* **9**, 1518 (1995).
9. M. Golembo, E. Raz, B.-Z. Shilo, *Development* **122**, 3363 (1996).
10. M. Freeman, C. Klämbt, C. S. Goodman, G. M. Rubin, *Cell* **69**, 963 (1992); R. Schweitzer, R. Howes, R. Smith, B.-Z. Shilo, M. Freeman, *Nature* **376**, 699 (1995); M. Golembo, R. Schweitzer, M. Freeman, B.-Z. Shilo, *Development* **122**, 223 (1996).
11. The activated monoclonal antibody to MAPK (dp-ERK) was raised against the 11–amino acid peptide His-Thr-Gly-Phe-Leu-Thr-(P_i)-Glu-Tyr-(P_i)-Val-Ala-Thr corresponding to the phosphorylated form of the ERK-activation loop.
12. The general rabbit polyclonal antibody to ERK (Ab. 7884) was generated against a 23–amino acid peptide from subdomain XI [K. C. Gause *et al.*, *J. Biol. Chem.* **268**, 16124 (1993)].
13. Y. Yung *et al.*, *FEBS Lett.* **408**, 292 (1997).
14. W. Biggs and S. L. Zipursky, *Proc. Natl. Acad. Sci. U.S.A.* **89**, 6295 (1992).
15. D2f (*8*) or Schneider cells were incubated with medium containing sSpitz for 12 min. After incubation the cells were lysed with sample buffer, and lysates were separated on a 12% SDS–polyacrylamide gel electrophoresis (PAGE) gel. After blotting to nitrocellulose, the general antibody to ERK was detected with a 1/10,000 dilution of Ab. 7884, and dp-ERK was detected with a 1/2000 dilution of anti–dp-ERK. For induction of dp-ERK in embryos, embryos containing *sev-hs-Gal4* and *UAS-secreted Spitz4a* were collected for 5 hours, administered heat shock at 37°C for 20 min, incubated at 29°C for 1 hour, and lysed. Control embryos of the same genotype were treated identically, but heat shock was eliminated.
16. Cells were fixed in 4% formaldehyde (fresh) for 20 min. After washes, the cells were permeabilized with 0.5% Triton X-100 in phosphate-buffered saline for 5 min. Subsequent steps were standard. Fresh embryos were fixed in 8% formaldehyde and kept in 100% methanol at −20°C. All washes were done with PBS, 0.1% Tween-20. In cases of DAB or fluorescent double stainings, the second primary antibody was added only after completion of washes of the secondary antibody to dp-ERK to ensure efficient staining and avoid cross-reactivity. All other aspects of staining were standard. After preincubation of anti–dp-ERK with the phosphorylated peptide antigen, staining was eliminated. Other antibodies used include rabbit anti–β-Gal (Cappel). Secondary antibodies include horseradish peroxidase–conjugated goat anti-mouse immunoglobulin G (IgG) and fluorescein isothiocyanate– or LRSC-conjugated goat anti-mouse IgG+IgM or anti-rabbit IgG (Jackson labs).
17. L. Gabay, R. Seger, B.-Z. Shilo, *Development* **124**, 3535 (1997).
18. E. Bier *et al.*, *Genes Dev.* **4**, 190 (1990).
19. A. L. Kolodkin, A. T. Pickup, D. M. Lin, C. S. Goodman, U. Banerjee, *Development* **120**, 1731 (1994).
20. Y. T. Ip, R. E. Park, D. Kosman, E. Bier, M. Levine, *Genes Dev.* **6**, 1728 (1992).
21. R. Noll, M. A. Sturtevant, R. R. Gollapudi, E. Bier, *Development* **120**, 2329 (1994); H. Xiao, L. A. Hrdlicka, J. Nambu, *Mech. Dev.* **58**, 65 (1996).
22. B. J. Rutledge, K. Zhang, E. Bier, Y. N. Jan, N. Perrimon, *Genes Dev.* **6**, 1503 (1992); P. zur Lage, Y. N. Jan, A. P. Jarman, *Curr. Biol.* **7**, 166 (1997); M. Okabe and H. Okano, *Development* **124**, 1045 (1997).
23. C. Klämbt, J. R. Jacobs, C. S. Goodman, *Cell* **64**, 801 (1991); E. Raz and B.-Z. Shilo, *Development* **114**, 113 (1992); H. Scholz, E. Sadlowski, A. Klaes, C. Klämbt, *Mech. Dev.* **62**, 79 (1997).
24. L. A. Perkins, I. Larsen, N. Perrimon, *Cell* **70**, 225 (1992); L. A. Perkins, M. R. Johnson, M. B. Melnik, N. Perrimon, *Dev. Biol.* **180**, 63 (1996).
25. M. A. Sturtevant *et al.*, *Genes Dev.* **7**, 961 (1993).
26. Fixation of imaginal discs was carried out in 4% formaldehyde for 30 min. Wash solutions contained 0.2% Triton X-100. In contrast to anti–dp-ERK staining of embryos, which is highly reproducible, staining of imaginal discs is variable, for unknown reasons.
27. B. Schnepp, G. Grumbling, T. Donaldson, A. Simcox, *Genes Dev.* **10**, 2302 (1996); A. A. Simcox *et al.*, *Dev. Biol.* **177**, 475 (1996).

28. We thank Y. Dolginov and D. Zharhary (Sigma Israel Chemicals, Rehovot, Israel) for help preparing activated antibody to MAPK (dp-ERK), and A. Brand, S. Crews, M. Freeman, W. Gehring, E. Hafen, C. Klämbt, M. Leptin, M. Levine, L. Perkins, and N. Perrimon for providing antibodies and fly stocks. We thank members of the Shilo lab, R. Schweitzer, and T. Volk for critical reading of the manuscript. R.S. is an incumbent of the Samuel and Isabela Friedman Career Development Chair. Supported by a grant from the Dr. Josef Cohn Minerva Center for Biomembrane Research (R.S.) and by grants from the Tobacco Research Council, US-Israel binational fund, UK-Israel binational fund, and Minerva Foundation (B.-Z.S.).

25 March 1997; accepted 7 July 1997

Thermophilic Fe(III)-Reducing Bacteria from the Deep Subsurface: The Evolutionary Implications

Shi V. Liu,* Jizhong Zhou, Chuanlun Zhang, David R. Cole, M. Gajdarziska-Josifovska, Tommy J. Phelps†

Thermophilic (45° to 75°C) bacteria that reduce amorphous Fe(III)-oxyhydroxide to magnetic iron oxides have been discovered in two geologically and hydrologically isolated Cretaceous- and Triassic-age sedimentary basins in the deep (>860 meters below land surface) terrestrial subsurface. Molecular analyses based on 16*S* ribosomal RNA (rRNA) gene sequences revealed that some of these bacteria represent an unrecognized phylogenetic group of dissimilatory Fe(III)-reducing bacteria. This discovery adds another dimension to the study of microbial Fe(III) reduction and biogenic magnetism. It also provides examples for understanding the history of Fe(III)-reducing microorganisms and for assessing possible roles of such microorganisms on hot primitive planets.

Dissimilatory Fe(III) reduction is proposed to be an early form of microbial respiration (*1*), and it may have influenced the geochemistry and the paleomagnetism of the Archaean Earth (*2*). Microbial Fe(III) reduction has been observed primarily in low-temperature environments that have been extensively influenced by modern surface processes (*3*). Previous studies on dissimilatory Fe(III)-reducing bacteria have been focused on mesophilic microorganisms within *Proteobacteria* (*4*), which are located distant from the deep branches on the phylogenetic tree (*5*). The paucity of information on thermophilic dissimilatory Fe(III)-reducing microorganisms (*6*) is striking in that thermophilic species are frequently found in many other groups of microorganisms such as methanogens, sulfate-reducing bacteria, and acetogens (*7*). This lack of information presents a difficulty in explaining microbial Fe(III) reduction on primitive Earth, which was reputedly warmer than Earth is now (*8*). Although the geological evidence for microbial Fe(III) reduction in Archaean Earth is recognized (*2*), the early evolution of microbial Fe(III)-reducing microorganisms on Earth has not yet been de-

S. V. Liu, J. Zhou, C. Zhang, T. J. Phelps. Environmental Sciences Division, Oak Ridge National Laboratory, Post Office Box 2008, Oak Ridge, TN 37831–6036, USA.
D. R. Cole. Chemical and Analytical Sciences Division, Oak Ridge National Laboratory, Post Office Box 2008, Oak Ridge, TN 37831–6110, USA.
M. Gajdarziska-Josifovska, Department of Physics, University of Wisconsin, Post Office Box 413, Milwaukee, WI 53201, USA.

*Present address: Department of Microbiology and Immunology, Allegheny University of the Health Sciences, Philadelphia, PA 19129, USA.
†To whom correspondence should be addressed.

lineated in biological studies.

We studied two geologically and hydrologically separated sedimentary basins, the Triassic-age Taylorsville Basin in Virginia and the Cretaceous-age Piceance Basin in Colorado. Geological and hydrological studies have shown that the deep portions of these basins have been isolated from surface processes for millions of years (9). The current temperature at the sampling depths (2652 to 2798 m below land surface) in the Taylorsville Basin ranges from 65° to 85°C, and the pore fluid pressure ranges from 30 to 35 MPa (9). The current temperatures at the three sampling depths (856 to 862 m, 1996 m, and 2090 to 2096 m below land surface) in the Piceance Basin were estimated to be 42°, 81°, and 85°C, respectively (9). Core samples were collected from tightly cemented, low-porosity arkosic silt stone and from organic-rich, laminated shale in the Triassic Taylorsville Basin, as well as from three geologic units in the Piceance Basin: one in the Tertiary Wasatch Formation and two in the Upper Cretaceous Williams Fork Formation (9). Drilling fluids were sampled from the fluid-receiving tank at different times during the drilling operation in the Piceance Basin. The sedimentary rock and drilling fluid samples were processed anaerobically and shipped on ice overnight to our laboratory for initiation of microbial incubations (*10*).

Enrichment cultures for thermophilic Fe(III)-reducing microorganisms were prepared with mineral media containing amorphous Fe(III) oxyhydroxide as an electron acceptor, and hydrogen (H_2) or short-chain fatty acids as the electron donors (*10*). Previous studies had shown that these substances are potentially available in deep terrestrial subsurface environments (*11*) and thus may be suitable substrates for deep-subsurface Fe(III)-reducing microorganisms. Within 1 to 2 weeks of inoculation with subsurface samples or enrichment cultures, black magnetic precipitates formed in incubation mixtures held at 60°C (Table 1). The Taylorsville Basin enrichment cultures used the fatty acids formate, acetate, and lactate as electron donors for Fe(III) reduction and magnetic mineral formation. The Piceance Basin enrichment cultures utilized H_2 and pyruvate as electron donors in addition to the above three fatty acids.

The formation of magnetic products was observed at temperatures between 45° and 75°C (Fig. 1) and at a salinity of 0 to 4% NaCl. In various uninoculated controls, significant abiotic Fe(III) reduction and magnetic product formation was not observed. Exposure of the thermophilic Fe(III)-reducing enrichment cultures to oxygen prevented the Fe(III) reduction, an indication of the anaerobic nature of the Fe(III)-reducing microorganisms. Furthermore, the thermophilic formation of magnetic iron oxides was prevented by the ferric reductase inhibitor *p*-chloromercuriphenyl sulfonate (*p*CMPS), the hydrogenase inhibitor quinacrine dihydrochloride, the protonophore carbonyl cyanide *m*-chlorophenylhydrazone (CCCP), and the electron transport inhibitors 2-*n*-heptyl-4-hydroxyquinoline-*N*-oxide (HOQNO) and dicumarol. The susceptibility of the thermophilic Fe(III)-reducing cultures to these metabolic inhibitors is consistent with a dissimilatory mechanism for Fe(III) reduction, which has been shown for mesophilic Fe(III)-reducing bacteria (*12*). The sulfate reduction inhibitor molybdate did not stop the Fe(III) reduction but shifted formation of reduced minerals from magnetite to siderite.

Magnetic precipitates (10 to 300 nm in size) were deposited extracellularly in association with microorganisms of different morphologies (Fig. 2A). The magnetic minerals were identified as a mixture of magnetite and maghemite crystallites on the basis of the lattice spacings revealed by selected area electron diffraction (Fig. 2B) and by high-resolution electron microscopy. Magnetite was the predominant phase. The existence of these two forms of

Table 1. Fe(III)-reducing and magnetic iron oxide-forming activities at 60°C in materials obtained from deep terrestrial subsurface environments (*21*).

Source of microorganisms	Activities with electron donor added into cultures*				
	Formate	Acetate	Lactate	Pyruvate	Hydrogen
Taylorsville Basin, sedimentary rocks	+	+	+	–	–
Piceance Basin, drilling fluids	+	+	+	+	+

*The plus sign indicates that Fe(III) reduction and magnetic mineral formation were observed within 5 days of incubation.

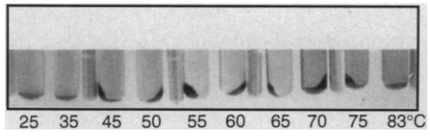

Fig. 1. Temperature profile of the microbial Fe(III)-reducing activity of the H_2-utilizing enrichment cultures from the Piceance Basin. After incubation for 5 days at the indicated temperatures, brown non-magnetic amorphous Fe(III) oxyhydroxides in the incubation tubes at 45° to 75°C became black and magnetic, and were attracted to the magnetic stirring bars taped to the outsides of incubation tubes during photographing. This caused the sloping of the precipitates toward the magnet side of the tube. Precipitates in incubation mixtures at 25°, 35°, and 83°C remained brown and non-magnetic at the end of incubation.

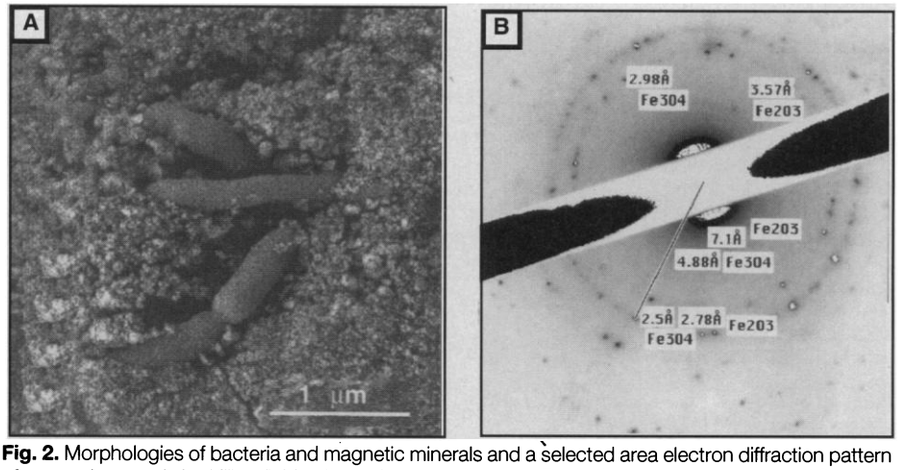

Fig. 2. Morphologies of bacteria and magnetic minerals and a selected area electron diffraction pattern of magnetic crystals in drilling fluid cultures from the Piceance Basin that were grown on H_2-CO_2-Fe(III) oxyhydroxide at 60°C. (**A**) SEM image of samples prepared anaerobically with minimum disturbance (*22*). (**B**) Selected area electron diffraction pattern of magnetic crystals. The presence of magnetite (Fe_3O_4) and maghemite (γ-Fe_2O_3) was indicated by black dots in the rings with characteristic *d*-spacings (*23*).

magnetic iron oxides in the magnetic precipitates was also confirmed by x-ray diffraction and Mössbauer spectroscopic analysis.

To further characterize the thermophilic Fe(III)-reducing enrichment cultures, we undertook a molecular analysis (*13*) of 16S rRNA genes. Community DNAs were extracted from the Fe(III)-reducing enrichment cultures incubated with nonfermentable substrates (H_2 and acetate) and from those with a fermentable substrate (pyruvate). The 16S rRNA genes were amplified and cloned into plasmid vectors, and the restriction fragment length polymorphism (RFLP) patterns of the clones were analyzed (*14*). Three dominant RFLP patterns were observed in various enrichment cultures (Table 2). RFLP patterns 1 and 2 were shared by enrichment cultures grown with nonfermentable and fermentable substrates, and the two patterns accounted for 43.6 to 54.6% of the clones. RFLP pattern 3 was observed in clones of H_2- and pyruvate-utilizing cultures but not in the acetate-utilizing culture.

The 16S rRNA gene sequences of representative clones bearing the three dominant RFLP patterns were analyzed (*15*). All of the sequences were affiliated with *Thermoanaerobacter* in the Gram-positive bacteria (Fig. 3) and (Table 2). The clones of RFLP patterns 1 and 3 were closely related to the *Thermoanaerobacter* species, bearing ~98% similarity (Table 2). The clones of the RFLP pattern 2, however, were most closely related to *T. ethanolicus* but had a 13% dissimilarity (Table 2). Such a degree of divergence in the 16S rRNA gene sequences suggests that the clones with RFLP pattern 2 may represent a previously unrecognized genus or family of bacteria (*16*).

From the analysis of the RFLP patterns in various cultures, we hypothesize that the microorganisms directly responsible for the dissimilatory Fe(III) reduction are those bearing RFLP pattern 2. This pattern was shared by Fe(III)-reducing microbial populations grown on three different electron donors. RFLP pattern 1 was also common to enrichment cultures grown on all three substrates. However, isolated bacteria such as TOR-39 (6) whose 16S rRNA sequences are highly similar to pattern 1 clones were unable to catalyze nonfermentative dissimilatory Fe(III) reduction. Bacteria bearing the RFLP pattern 3 might play some role in the Fe(III)-reduction in the hydrogen- and pyruvate-grown cultures. However, bacteria with this RFLP pattern are unlikely candidates for producing the observed dissimilatory Fe(III) reduction; this RFLP pattern was absent from acetate-grown cultures and the clones with this pattern were highly similar in 16S rRNA gene sequences to those of fermentative *Thermoanaerobacter* species. However, further studies are necessary to delineate the respective roles of the various bacteria in thermophilic Fe(III) reduction.

The discovery of these forms of thermophilic Fe(III)-reducing bacteria described above has broad implications regarding the evolution of Fe(III)-reducing microorganisms and biogenic contributions to paleomagnetism. A wide phylogenetic distribution of Fe(III)-reducing bacteria, including mesophilic and thermophilic species, could reflect the early evolution of Fe(III) respiration because early evolved characteristics tend to be conserved among widely distributed descendants (*17*). Furthermore, the existence of thermophilic Fe(III)-reducing bacteria in geologically isolated, millions-of-years-old thermal regimes suggests that thermophily may be an ancestral feature associated with Fe(III)-reduction. The ability of microorganisms to produce magnetic iron oxides from amorphous Fe(III) oxyhydroxide at high temperatures expands the biotope boundary for microbial Fe(III)-reducing activities. This capability also supports the theory that biogenic magnetism may have occurred in Archaean banded iron formations that formed at high temperatures (55° to 76°C) (*18*).

The discovery of thermophilic Fe(III)-reducing bacteria on Earth may also have implications for studying exobiology on, for example, Mars: the recent finding of putative biogenic magnetite in an ancient martian meteorite (*19*) raises the possibility that Fe(III)-reducing microorganisms evolved not only on Earth but also elsewhere. Early Mars and early Earth might have exhibited similar hydrothermal activities compatible with life (*20*). Thus, thermophily may have been a common feature of the early evolved forms of Fe(III)-reducing bacteria.

Table 2. The dominant RFLP patterns and 16S rRNA gene sequence similarity of the 16S rDNA clones in thermophilic Fe(III)-reducing enrichment cultures grown with different electron donors. The numbers in parentheses are percentages of the total clones.

Dominant RFLP patterns	Representative clones in cultures with different electron donors			Most similar species	Sequence similarity (%)
	Hydrogen	Acetate	Pyruvate		
1	H-2 (30.8)	A-3 (37.1)	P-9 (24.3)	*T. ethanolicus*	97.9
2	H-3 (19.0)	A-10 (19.0)	P-3 (19.3)	*T. ethanolicus*	86.7
3	H-5 (14.3)	ND*	P-1 (20.7)	*T. brockii*	97.7

*ND = not detected.

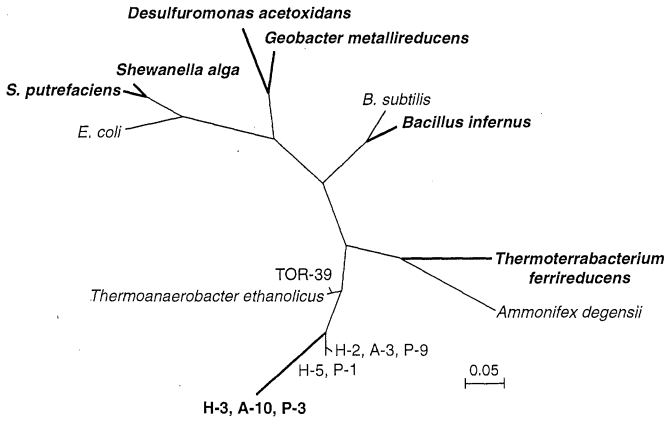

Fig. 3. The phylogenetic relation between the newly discovered thermophilic Fe(III)-reducing bacteria (bold Roman letters connected with a thick line) and other examples of Fe(III)-reducing bacteria (italic letters connected with thick lines). This relation is deduced from 16S rRNA gene sequencesof the bacteria. The letters H, A, and P indicate the hydrogen-, acetate-, and pyruvate-utilizing cultures, respectively. The numbers after the hyphens specify the clones (Table 2). The scale bar represents 0.05 nucleotide change per position.

REFERENCES AND NOTES

1. D. R. Lovley, *Microbiol. Rev.* **55**, 259 (1991); K. H. Nealson and C. R. Myers, *Am. J. Sci.* **290A**, 35 (1990).
2. E. C. Perry, F. C. Tan, G. B. Morey, *Econ. Geol.* **68**, 1110 (1973); J. C. G. Walker, *Nature* **309**, 340 (1984); R. Becker and R. Clayton, *Geochim. Cosmochim. Acta* **36**, 577 (1972); M. E. Baur, J. M. Hayes, S. A. Studley, M. R. Walter, *Econ. Geol.* **80**, 270 (1985); D. A. Brown, G. A. Gross, J. A. Sawicki, *Can. Mineral.* **33**, 1321 (1995).
3. D. R. Lovley, *Annu. Rev. Microbiol.* **47**, 263 (1993); K. H. Nealson and D. Saffarini, *Annu. Rev. Microbiol.* **48**, 311 (1994).
4. D. J. Lonergan, H. Jenter, J. D. Coates, T. M. Schmidt, D. R. Lovley, *J. Bacteriol.* **178**, 2402 (1996).
5. C. R. Woese, *Microbiol. Rev.* **58**, 1 (1994); G. J. Olsen, C. R. Woese, R. Overbeek, *J. Bacteriol.* **176**, 1 (1994).

6. T. D. Brock and J. Gustafson, *Appl. Environ. Microbiol.* **32**, 567 (1976); D. R. Boone *et al.*, *Int. J. Syst. Bacteriol.* **45**, 441 (1995); .A. Slobodkin *et al.*, *Doklady Akad. Nauk* **345**, 694 (1995); C. Zhang *et al.*, *Appl. Biochem. Biotechnol.* **57/58**, 923 (1996); A. C. Greene, B. K. C. Patel, A. J. Sheehy, *Int. J. Syst. Bacteriol.* **47**, 505 (1997); A. Slobodkin, A.-L. Reysenbach, N. Strutz, M. Dreier, J. Wiegel, *ibid.*, p. 541.
7. K. O. Stetter, G. Fiala, G. Huber, R. Huber, A. Segerer, *FEMS Microbiol. Rev.* **75**, 117 (1990); K. O. Stetter, *ibid.* **18**, 149 (1996).
8. H. Ohmoto and R. P. Felder, *Nature* **328**, 244 (1987); J. F. Kasting and T. P. Ackerman, *Science* **234**, 1383 (1986); J. F. Kasting, *Precamb. Res.* **34**, 205 (1987); *Science* **259**, 920 (1993).
9. D. L. Balkwill *et al.*, *Eos* **75**, 390 (1994); H.-Y. Tseng, T. C. Onstott, R. C. Burruss, D. S. Miller, *Chem. Geol.* **127**, 297 (1996); J. K. Pitman, W. W. Dickinson, in *U.S. Geological Survey Bulletin*, No. 1886 (1986), pp. J1–J15; R. C. Johnson, D. D. Rice, *Bull. Am. Assoc. Petrol. Geol.* **74**, 805 (1990).
10. Original enrichment cultures were initiated by inoculating samples at a 1:10 ratio into a basal medium [C. Zhang *et al.*, *Appl. Biochem. Biotechnol.* **57/58**, 923 (1996)] containing 1% (wt/v) NaCl, 70 mM amorphous Fe(III)-oxyhydroxide as an electron acceptor, and 10 mM of a short-chain fatty acid (formate, acetate, lactate, or pyruvate) or 80% H_2 (balanced with 20% CO_2 and at 1 atm. gas pressure) as an electron donor. The incubations were at 60°C (in the dark without shaking).
11. J. C. G. Walker, *Nature* **329**, 710 (1987); A. F. Trendall and R. C. Morris, Eds., *Iron-Formation: Facts and Problems* (Elsevier, Amsterdam, 1983); P. B. McMahon and F. H. Chapelle, *Nature* **349**, 233 (1991); B. N. Bjornstad *et al.*, *Ground Water Monitoring Remediation* **14**, 140 (1994).
12. R. G. Arnold, T. J. DiChristina, M. R. Hoffmann, *Appl. Environ. Microbiol.* **52**, 281 (1986); C. R. Myers and K. H. Nealson, *J. Bacteriol.* **172**, 6232 (1990); C. R. Myers and J. M. Myers, *FEMS Microbiol. Lett.* **108**, 15 (1993); *J. Appl. Bacteriol.* **76**, 253 (1994); Y. A. Gorby and D. R. Lovley, *Appl. Environ. Microbiol.* **57**, 867 (1991).
13. S. M. Barns, R. E. Fundyga, M. W. Jeffries, N. R. Pace, *Proc. Natl. Acad. Sci. U.S.A.* **91**, 1609 (1994); D. M. Ward, M. M. Bateson, R. Weller, A. L. Ruff-Roberts, *Adv. Microb. Ecol.* **12**, 219 (1992); J. A. Fuhrman, K. McCallum, A. A. Davis, *Nature* **356**, 148 (1992).
14. Genomic DNAs were extracted from the cells harvested from the enrichment cultures by means of the freezing-thawing and SDS lysis methods [J.-Z. Zhou *et al.*, *Appl. Environ. Microbiol.* **62**, 461 (1996)]. The 16*S* rRNA genes were amplified and cloned into the pCR™II TA cloning vector. The 16*S* rRNA gene inserts were detected by RFLP analysis with four tetrameric restriction enzymes: Msp I plus Rsa I and Hha I plus Hae III.
15. The 16*S* rRNA genes were partially sequenced with the reverse primer spanning *E. coli* 16*S* rRNA gene positions of 529–512 by means of an automatic fluorescent sequencer [J.-Z. Zhou *et al.*, *Int. J. Syst. Bacteriol.* **45**, 500 (1995)]. The phylogenetic tree was constructed by the maximum likelihood method with the program fastDNAml in EDP [N. Larsen *et al.*, *Nucleic Acids Res.* **21**, 3021 (1993)].
16. D. R. Boone, W. B. Whitman, P. Rouviere, In *Methanogenesis: Ecology, Physiology, Biochemistry, and Genetics*, J. G. Ferry, Ed. (Chapman & Hall, New York, 1993), pp. 35–80; N. K. Fry, S. Warwick, N. A. Saunders, T. M. Embley, *J. Gen. Microbiol.* **137**, 1215 (1991); R. Devereux *et al.*, *J. Bacteriol.* **172**, 3609 (1990); F. E. Dewhirst, B. J. Paster, I. Olsen, G. J. Fraser, *ibid.* **174**, 2002 (1992).
17. C. R. Woese, *Microbiol. Rev.* **51**, 221 (1987); C. R. Woese, O. Kandler, M. L. Wheelis, *Proc. Natl. Acad. Sci. U.S.A.* **87**, 4576 (1990).
18. L. P. Knauth and S. Epstein, *Geochim. Cosmochim. Acta* **40**, 1095 (1976); L. P. Knauth and D. R. Lowe, *Earth Planet. Sci. Lett.* **41**, 209 (1978); B. L. Winter and L. P. Knauth, *Precamb. Res.* **59**, 283 (1992).
19. D. S. McKay *et al.*, *Science* **273**, 924 (1996).
20. S. W. Squyres and J. F. Kasting, *ibid.* **265**, 744 (1994).
21. Fe(III) reduction was monitored by measuring the accumulation of Fe(II) by the ferrozine method [C. Zhang *et al.*, *Appl. Biochem. Biotechnol.* **57/58**, 923 (1996)]. Formation of magnetic minerals was visually inspected with a magnet and was confirmed by x-ray diffraction.
22. Slides for scanning electron microscopy were made by transferring undisturbed solid material to the poly-L-lysine–coated cover glass and fixed with 2.5% (by volume) glutaraldehyde (1 hour) and 2% $KMnO_4$ (30 min) at room temperature. The samples were then dehydrated with an ethanol series under aerobic conditions, air-dried, and coated with gold-palladium.
23. The *d*-spacings at 2.53 Å, 1.48 Å, 2.98 Å, 4.88 Å, 2.10 Å, and 1.71 Å and their intensities are shared by both magnetite (Fe_3O_4) and maghemite (the γ-Fe_2O_3 spinel) within the resolution limits of the electron diffraction technique. The *d*-spacings at 7.1 Å, 3.57 Å, and 2.78 Å are characteristic of maghemite.

24. We thank D. Coffey (ORNL; scanning electron microscopy), E. Voelkl (ORNL; transmission electron microscopy), W. R. Dunham and N. Moon (Univ. of Michigan; Mössbauer spectroscopy) for collaborative efforts, and A. V. Palumbo (ORNL) for discussion. Supported by the Subsurface Science Program managed by F. J. Wobber and the Geosciences Research Program of U.S. Department of Energy contracted to Lockheed Martin Energy Research Corp.; the ORNL Postdoctoral Research Associates Program administered jointly by ORNL and Oak Ridge Institute for Science and Education (S. V. Liu, J. Zhou, and C. Zhang); the ORNL Laboratory-Directed Research and Development Program; and the ORNL High-Temperature Materials Laboratory summer faculty fellowship program (M.G.J.).

28 October 1996; accepted 11 June 1997

Altered Neural Cell Fates and Medulloblastoma in Mouse *patched* Mutants

Lisa V. Goodrich, Ljiljana Milenković, Kay M. Higgins, Matthew P. Scott*

The *PATCHED* (*PTC*) gene encodes a Sonic hedgehog (Shh) receptor and a tumor suppressor protein that is defective in basal cell nevus syndrome (BCNS). Functions of *PTC* were investigated by inactivating the mouse gene. Mice homozygous for the *ptc* mutation died during embryogenesis and were found to have open and overgrown neural tubes. Two Shh target genes, *ptc* itself and *Gli*, were derepressed in the ectoderm and mesoderm but not in the endoderm. Shh targets that are, under normal conditions, transcribed ventrally were aberrantly expressed in dorsal and lateral neural tube cells. Thus Ptc appears to be essential for repression of genes that are locally activated by Shh. Mice heterozygous for the *ptc* mutation were larger than normal, and a subset of them developed hindlimb defects or cerebellar medulloblastomas, abnormalities also seen in BCNS patients.

The human *PTC* gene is a tumor suppressor and developmental regulator (*1*). Some patients with BCNS have germline mutations in *PTC* and are at increased risk for developmental defects such as spina bifida and craniofacial abnormalities, basal cell carcinoma of the skin, and brain tumors (*2*). *PTC* mutations also occur in sporadic basal cell carcinomas (*1*), which generally have both copies of *PTC* inactivated.

In the fruit fly *Drosophila*, Ptc is a key component of the Hedgehog (Hh) signaling pathway, which controls cell fate determination during development (*3*). Hh protein, secreted from localized regions, antagonizes the actions of its apparent receptor, Ptc, in nearby cells (*4*). In the absence of a Hh signal, Ptc represses transcription of multiple target genes, including *ptc* itself, *wingless* (a *Wnt* gene), and the *transforming growth factor* β–related gene *decapentaplegic*. In flies, *ptc* mutations cause derepression of target genes, cell fate changes, and excessive growth in some tissues (*5*). Hh induces a high level of *ptc* transcription by inhibiting the function of Ptc protein, so paradoxically an abundance of *ptc* transcript is an indicator of a low level of Ptc function. Vertebrate *ptc* expression is also regulated by Hh proteins (*6*), which can bind directly to Ptc (*7*).

The role of the Hh-Ptc pathway in skin cancer has been established by BCNS studies and with a mouse model (*8*), but less is known about the brain tumors associated with BCNS. About 3% of BCNS patients develop medulloblastomas (*9*), cerebellar tumors that usually arise in young children and have a mortality rate of ~50% (*10*). *ptc* mutations have been detected in sporadic medulloblastomas (*11*), but this tumor type is rare and there are few clear animal models (*12*), so much remains to be learned about its origins and biology.

To study the roles of *ptc* in development and in tumorigenesis, we constructed mice

Departments of Developmental Biology and Genetics and the Howard Hughes Medical Institute, Stanford University School of Medicine, Stanford, CA 94305–5427, USA.

*To whom correspondence should be addressed. E-mail: scott@cmgm.stanford.edu